

# Thin double layer approximation to describe streaming current fields in complex geometries: Analytical framework and applications to microfluidics

Edouard Brunet<sup>1</sup> and Armand Ajdari<sup>2,\*</sup><sup>1</sup>Laboratoire MMN, UMR CNRS-ESPCI 7083, 10 rue Vauquelin, F-75231 Paris Cedex 05, France<sup>2</sup>Laboratoire de Physico-Chimie Théorique, UMR CNRS-ESPCI 7083, 10 rue Vauquelin, F-75231 Paris Cedex 05, France

(Received 28 December 2005; published 16 May 2006)

We set up an analytical framework that allows one to describe and compute streaming effects and electro-osmosis on an equal footing. This framework relies on the thin double layer approximation commonly used for description of electroosmotic flows, but rarely used for streaming problems. Using this framework we quantitatively assess the induction of bulk streaming current patterns by topographic or charge heterogeneities on surfaces. This too also permits analytical computation of all linear electrokinetic effects in complex microfluidic geometries, and we discuss a few immediate applications.

DOI: [10.1103/PhysRevE.73.056306](https://doi.org/10.1103/PhysRevE.73.056306)

PACS number(s): 47.60.+i, 47.65.-d, 47.56.+r, 85.85.+j

## I. INTRODUCTION

The development of microfluidic systems in the last decade has triggered a renewed interest in electrokinetics, in answer to both applied and fundamental demand. Indeed, electrically generated flows have been shown to be of great use for many lab-on-a-chip applications, and a proper understanding of those is a requirement for the proper design of the systems [1–5]. On the fundamental side, the development of microfabrication methods to produce well controlled surfaces, together with the microfluidic format for performing experiments, puts one in a better position to test the many theoretical works on electrokinetics, in contrast to more conventional studies of electrophoretic mobilities on not so cleanly defined colloids, or of streaming potentials on difficultly controllable porous media. This cross interest in applied and fundamental aspects is further enhanced by the parallel development of numerical methods that allow more exhaustive studies, both at the fundamental scale where these phenomena are generated (the electric double layer) [6,7], but also at the scale of the microfluidic channel in which the flow develops [8–11].

A specific subclass in this whole field is the analysis and use of electrokinetic phenomena in geometries brought in by the development of microfluidic devices (Fig. 1), which includes in particular patterned heterogeneous surfaces. Here again microfabrication has changed the paradigm from studying the effects of unwanted defects to taking advantage of the many methods available to produce surfaces with controlled patterns of surface chemistry, charge, or/and topography. The clever use of such surfaces allows one to design electro-osmotic flows with various geometrical features (vortices, two-way flows, etc.) [12–17], with potential functionalities such as mixing. Such features also induce hydrodynamic dispersion in transport or electrophoresis experiments. Patterns of specific symmetries can be used to generate transverse effects, allowing, for example, pumping in a channel by application of a dc field transverse to the channel [18].

The complexity of the underlying physics has mostly confined the theoretical analysis of electrokinetic effects in such patterned geometries to three kinds of methods: lubrication analysis for slowly varying heterogeneities [23], numerical methods [8–11,15–17,21], and analysis of electro-osmosis using the “thin double layer” + “weak surface potential” approximation [13,24]. This last approximation, although in principle limited by the range of validity of its underlying hypothesis, has proved to be a very powerful way to investigate semiquantitatively essential features of electro-osmotic flows in many geometries [8–10,13,24]. Its power stems from the decoupling between the computation of electric and hydrodynamic effects: one solves for the electric field first, and then faces a purely hydrodynamic problem with an effective slip boundary condition for the flow that depends on the former computation of the electric field [24].

In this paper, we extend this powerful last method, used up to now only for electro-osmosis, to the other half of the electrokinetics phenomenology, namely streaming effects (electric effects induced by hydrodynamic flows). Indeed, from a fundamental point of view, both phenomena (electro-osmosis and streaming effects) should be approached in a combined unified frame [25].

We correspondingly introduce in Sec. II the system of equations adequate to approach systematically electrokinetics problems in arbitrary geometry, within the thin double

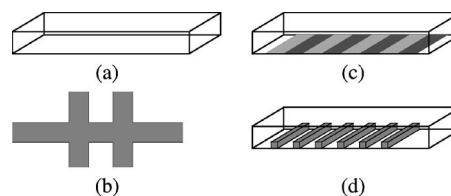


FIG. 1. Typical geometries for the study of electrokinetic effects: (a) the classical geometry of a straight and homogeneous channel [19], (b)–(d) example of geometries brought in by the development of microfluidics. (b) channel topology of a capillary electrophoresis injection device [20], (c) microchannel with patterned surface charges [12], (d) microchannel with patterned topography [21,22].

\*Electronic address: [armand@turner.pct.espci.fr](mailto:armand@turner.pct.espci.fr)

layer (TDL)+ weak surface potential (WSP) approximation.

We then report in Sec. III a check of the consistency of this formalism by showing that it yields Onsager's reciprocity relations for global quantities, relations that the authors have shown to hold in a more general context, i.e., when the constraints of weak surface potential and thin double layer are lifted [26].

We then illustrate the power of this formalism in Sec. IV by computing electro-osmosis and streaming effects in model microfluidic geometries involving stripe patterns. Such geometries have been shown in previous theoretical and experimental studies to be appropriate paradigms to understand the effects of surface heterogeneities and the corresponding microfluidic functionalities [5]. Indeed our analysis unveils interesting qualitative features, such as the generation of bulk electric currents induced by an applied pressure drop. It also allows us to quantitatively assess the importance of transverse effects in channels with patterns at an angle with the channel axis. We recover in the appropriate limits results from earlier analytical studies. For the sake of clarity and readability, most of the explicit results for the various geometries considered in this section are postponed to compact appendixes.

Eventually we close in Sec. V, with a discussion of perspectives emanating from this analysis, that could trigger experimental and numerical studies.

## II. GENERAL FORMALISM FOR THE THIN DOUBLE LAYER+WEAK SURFACE POTENTIAL APPROXIMATION

### A. Electrokinetic effects in a flat homogeneous geometry

To set the stage for the following and to clarify the physics at work, we start by recalling the textbook description of the electrokinetic effects on top of a flat, nonconducting and homogeneously charged surface (see, e.g., Hunter [27]). We consider the surface immersed in an electrolyte solution of viscosity  $\eta$ , dielectric constant  $\varepsilon$ . It acquires in contact with the electrolyte a homogeneous surface charge corresponding to an equilibrium surface potential  $\zeta$  on the plane  $z=0$  where the fluid velocity is supposed to go down to zero at very small scale (no-slip boundary condition). The ion concentrations  $c_i^{eq}$  and the electrostatic potential  $\phi^{eq}$  in the solution at equilibrium obey the Poisson equation  $\varepsilon\Delta\phi + \sum_i q_i c_i^{eq} = 0$ , where  $q_i$  is the charge of ions of type  $i$ . Requiring thermal equilibrium yields then the classical description for the structure of the outer part of the electric double layer (EDL), and its characteristic thickness  $\lambda_D = (\varepsilon k_B T / \sum_i q_i^2 c_i^{eq})^{1/2}$ .

Although this layer is very thin (typically  $\lambda_D \sim 1 - 100$  nm), the fact that the solution is non-neutral there leads to coupling between hydrodynamics and electric effects. The two classical resulting phenomenologies (electrokinetic effects) are electro-osmosis and streaming current that we describe in that order.

If an electric current is applied along the surface, so that there is an electric field  $\mathbf{E} = Ex$  parallel to the wall in the solution, then a net force is applied to the fluid where its is charged, as described by the force balance along the  $x$  direction,

$$\eta \frac{\partial^2 v_x}{\partial z^2} + \sum_i c_i^{eq} q_i E = 0 \quad (1)$$

with  $z$  normal to the wall, and  $v$  the fluid velocity. There is no pressure gradient because the geometry is translationally invariant along  $x$ . Combining the Poisson equation with the no-slip boundary condition and a no applied stress condition ( $\eta \partial_z v_x = 0$ ) at large values of  $z$  yields

$$v_x = \frac{\varepsilon}{\eta} (\phi^{eq} - \zeta) E. \quad (2)$$

This flow is called electro-osmosis. The velocity increases from zero on the wall to a finite homogeneous constant value beyond the thin double layer:

$$v_{eo} = - \frac{\varepsilon \zeta}{\eta} E. \quad (3)$$

If one is interested only in the flow at scales much larger than  $\lambda_D$ , an appropriate description is this "outer" solution: the fluid "slips" as a plug on the surface at the velocity  $v_{eo}$ .

Streaming effects correspond to the electric effects generated by a hydrodynamic flow. In the present geometry, consider a shear flow  $v_x = \dot{\gamma} z$  applied on top of the plate. This convects the liquid and thus generates an electric current wherever the charge density is nonzero, i.e., within the double layer.

$$j = \sum_i q_i c_i^{eq} v_x. \quad (4)$$

Therefore the electric current is parallel to the plates and confined to the  $\lambda_D$ -thick layer. Again if one is not interested in the fine spatial structure of this current, but rather in a larger scale description, then the flow seems to generate a surface current (the "streaming current"), of amplitude given by  $J_s = \int_0^\infty dz \sum_i q_i c_i^0 v_x$ . Using Poisson equation, this effective surface current is easily shown to be

$$J_s = - \varepsilon \zeta \dot{\gamma}. \quad (5)$$

where  $\dot{\gamma}$  is the shear rate (homogeneous in the present problem).

Clearly both electrokinetic effects originate within the double layer and both can be described at larger scales by the effective equations (3) and (5).

### B. Applying the TDL and WSP approximations

Given the experimentally small values of the Debye length  $\lambda_D$  (typically microns), it is often tempting to use the previous picture to describe phenomena *locally*, i.e., at a scale intermediate between  $\lambda_D$  and the scales characteristic of the geometry of interest. For this to be applicable (TDL approximation) every typical length within the system has to be larger than the Debye length  $\lambda_D$ . This concerns

(i) the channel transverse dimensions, so that the double layers are fully developed and that an effective interfacial description can be used,

(ii) the length scale of the variations of the surface charge (or potential), so that the surface can *locally* be described as homogeneously charged,

(iii) the length scale of the variation in topography or geometry of the surface, so that it can be *locally* described as flat.

Additional requirements hold to apply the previous picture in all its simplicity. Indeed, Eqs. (3) and (5) were derived assuming no perturbation of the distribution of ions with respect to equilibrium, which holds true in the simple infinite flat homogeneous geometry. In more general geometries, this will hold only if the surface potential remains moderate, which we describe by weak surface potential approximation (WSP). In the present frame where we focus on thin double layers, this approximation is not so restrictive as requesting  $\zeta \ll k_B T$ . Indeed, and although a specific analysis should be performed for each geometry, the restriction in many situations will take a form similar to that appearing in the study of the electrophoresis of a homogeneous spherical particle (see, for example, the very nice review of Anderson [24]), namely  $(\lambda_D/a)\tanh(e\zeta/2k_B T) \ll 1$ , with  $a$  a typical dimension over which a property of the geometry changes (the radius of the spherical particle for that problem). This is somewhat less restrictive than  $e\zeta/k_B T \ll 1$ , since this length has already been assumed to be much larger than  $\lambda_D$ .

Once these approximations are made, one can apply the effective equations (3) and (5) and decouple the computations of the electric and hydrodynamic flow fields. Note that as we assume weak surface potentials, we will typically neglect effects often called “electroviscous,” whereby the original driving field (electric or hydrodynamic) generates a primary electrokinetic effect (electro-osmosis or streaming current), which in turn generates a secondary electrokinetic effect that leads to a correction to the original driving field (an electric current or a hydrodynamic flow). Indeed such corrections obviously scale at most as  $(e\zeta/k_B T)^2$ , and will be negligible in the present frame compared to the direct electrokinetic effects scaling as  $e\zeta/k_B T$ .

Then our formalism simply falls into two separate parts: the classical one that has been used by many authors to describe electro-osmosis [24], and one for the description of streaming effects on the same footing that we introduce here. All quantities in the former problem will be denoted by  $(e)$  subscripts to recall that the effects are electrically driven, whereas  $(p)$  subscripts will be used in the second case to remind that the effects are pressure driven.

### C. Electrically driven flows

With the above-mentioned approximations the coupling between the electric and hydrodynamic problems solely appears through interfacial boundary conditions. In addition, the WSP approximations guarantees that the thin double layer is not particularly conducting with respect to the bulk, so that to quantify electro-osmosis, one first solves for the electric field in the solution using the Laplace equation as the conductivity is homogeneous:

$$\nabla^2 \phi^{(e)} = 0, \quad (6)$$

$$\mathbf{j}^{(e)} \cdot \mathbf{n} = 0 \quad (7)$$

with  $\mathbf{n}$  the normal to the wall, taken in the following arbitrarily pointing inwards (i.e., from the wall into the solution).

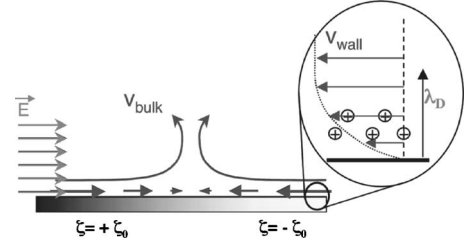


FIG. 2. Planar wall with a nonhomogeneous  $\zeta$  potential. The electrical field  $E$  induces a nonhomogeneous slip velocity which in turn induces recirculation flows in the bulk.

The boundary condition used above corresponds to no current entering or leaving the walls.

Once the tangential electrical field is obtained, its effect on the flow can be described following Sec. II A as slip velocity is given by  $\mathbf{v}_s^{(e)} = \mu(-\nabla \phi_s^{(e)})$  with  $\mu = -\epsilon\zeta/\eta$  the (potentially position dependent) *local* electroosmotic mobility and  $(-\nabla \phi_s^{(e)})$  the *local* tangential electric field.

The pattern of slip velocities gives rise to a bulk velocity field  $\mathbf{v}^{(e)}$  (and a pressure field  $p^{(e)}$ ) that can be derived using Stokes equation and volume conservation:

$$\eta \nabla^2 \mathbf{v}^{(e)} - \nabla p^{(e)} = 0, \quad (8)$$

$$\nabla \cdot \mathbf{v}^{(e)} = 0, \quad (9)$$

$$\mathbf{v}_s^{(e)} = -\mu \nabla \phi_s^{(e)}. \quad (10)$$

Note that we focus here on steady-state problems, but situations where the applied electric field changes in time can be dealt with similarly, with the addition of the vorticity diffusion term to Eq. (8).

The procedure (6)–(10) is a now standard protocol for the study of electro-osmotic flows in nonhomogeneous geometries such as the simple one described in Fig. 2.

### D. Streaming currents

In a symmetric way, application of a pressure field yields at zeroth order a velocity field given by Stokes law:

$$\eta \nabla^2 \mathbf{v}^{(p)} - \nabla p^{(p)} = 0, \quad (11)$$

$$\nabla \cdot \mathbf{v}^{(p)} = 0, \quad (12)$$

$$\mathbf{v}_s^{(p)} = \mathbf{0}. \quad (13)$$

with a no-slip boundary condition on the wall.

As the charged double layer is very thin, this flow field induces “effective” surface streaming currents that depend on the local shear rate [as described by Eq. (5)] Given the arbitrariness of the geometry the result must be written in tensorial form:

$$\mathbf{j}_s^{(p)} = -\epsilon\zeta(\mathbf{n} \cdot [(\nabla \mathbf{v}^{(p)})^t + \nabla \mathbf{v}^{(p)}] \cdot \mathbf{T}) = \mu \mathbf{n} \cdot \sigma^{(p)} \cdot \mathbf{T} \quad (14)$$

with  $\mathbf{T} = [\mathbf{I} - \mathbf{nn}]$  the projection operator on the plane locally tangent to the surface, and  $\sigma^{(p)} = -p^{(p)}\mathbf{I} + \eta[(\nabla \mathbf{v}^{(p)})^t + \nabla \mathbf{v}^{(p)}]$  the hydrodynamic stress tensor, and again  $\mu = -\epsilon\zeta/\eta$  the *lo-*

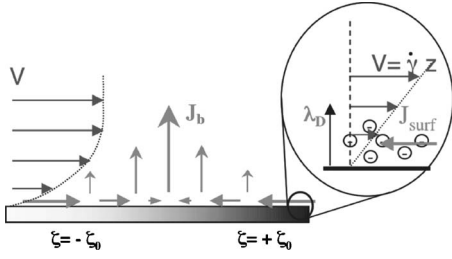


FIG. 3. Planar wall with a nonhomogeneous  $\zeta$  potential. The pressure driven flow  $V$  induces a nonhomogeneous surface streaming current  $J_s$  (inside the Debye layer). This leads to injection of a bulk current  $J_b$ .

*cal* parameter describing the surface charge (the local electroosmotic mobility).

How does this boundary condition couples to the electric-field pattern in the bulk? In an arbitrary geometry, the above streaming surface current varies from place to place which requires injection or removal of charges into the interfacial layer (Fig. 3). Mathematically, charge conservation implies that a *bulk* electric current  $\mathbf{j}_b^{(p)}$  is generated, that obeys close to the wall the conservation equation

$$\nabla_s \cdot \mathbf{j}_s^{(p)} + \mathbf{j}_b^{(p)} \cdot \mathbf{n} = 0 \quad (15)$$

with  $\nabla_s \cdot \mathbf{j}_s^{(p)}$  the surface divergence of the surface current.

Therefore the whole phenomenology of streaming effects is that the applied pressure drop (or flow) generates both surface currents as described by Eq. (14) and *bulk effects* through Eq. (14): a bulk current  $\mathbf{j}_b^{(p)}$ , and the related electric potential  $\phi^{(p)}$  and field  $\mathbf{E}^{(p)} = -\nabla \phi^{(p)}$ , given by

$$\Delta \phi_b^{(p)} = 0, \quad (16)$$

$$\mathbf{j}_b^{(p)} = -\gamma_{el} \nabla \phi^{(p)} \quad (17)$$

with the boundary conditions (14) and (15).  $\gamma_{el}$  denotes the bulk conductivity.

The set of equations (11)–(17) is the procedure to be used in an arbitrary geometry to determine streaming effects, within the TDL+WSP approximation. It is the natural counterpart of the common procedure for electro-osmosis (6)–(10), and constitutes the fundamental result of this paper.

In the remaining part of this paper we make use of this result. We first demonstrate Onsager's reciprocity relations for arbitrary geometry within this framework. We then compute flow and field structures for a variety of geometries relevant for microfluidics, before emphasizing a few more direct practical interests of the present approach.

### III. RECIPROCITY RELATIONS

We show in this section how one can recover generalized forms of the Onsager reciprocity relations for electrokinetic effects within this particular framework. The strategy is rather similar to the one we used in a previous work to demonstrate those relations more generally [26]. Thanks to the approximations made, the derivation is, however, logically much simplified.

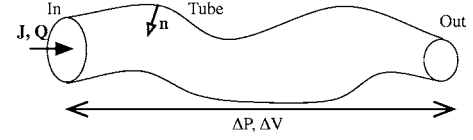


FIG. 4. Capillary of arbitrary geometry and surface charge, with two ports denoted *in* and *out*, and an internal wall designed by *tube*.  $J$ ,  $Q$ ,  $\Delta P$ , and  $\Delta V$  are respectively the total current, the flow rate, the pressure drop, and the electrical potential drop.

For the sake of clarity we focus on a capillary geometry with only two ports (*in* and *out*) as depicted in figure (Fig. 4). The geometry of the capillary and the distribution of surface potential is arbitrary. Generalization to geometries with more than two inlets is straightforward following the strategy of Ref. [26].

The demonstration starts with relations between the bulk solutions of the electrically driven problem  $^{(e)}$  and that of the hydrodynamically driven one  $^{(p)}$ , in the spirit of the reciprocal theorems often used for low-Reynolds-number hydrodynamics. From the sets of equations (6)–(17), the hydrodynamic stress tensors  $\boldsymbol{\sigma}^{(e),(p)}$  and velocity fields obey

$$\nabla \cdot (\boldsymbol{\sigma}^{(p)} \cdot \mathbf{v}^{(e)}) = \nabla \cdot (\boldsymbol{\sigma}^{(e)} \cdot \mathbf{v}^{(p)}) \quad (18)$$

while the potentials and currents satisfy

$$\nabla \cdot (\phi^{(p)} \cdot \mathbf{j}_b^{(e)}) = \nabla \cdot (\phi^{(e)} \cdot \mathbf{j}_b^{(p)}) \quad (19)$$

We subtract the two previous equalities and integrate over the fluid volume within the capillary. Transforming the volume integrals into surface ones (over the walls+ports), we get

$$\int \int \mathbf{n} \cdot (\boldsymbol{\sigma}^{(p)} \cdot \mathbf{v}^{(e)} - \phi^{(p)} \cdot \mathbf{j}_b^{(e)}) \int \int \mathbf{n} \cdot (\boldsymbol{\sigma}^{(e)} \cdot \mathbf{v}^{(p)} - \phi^{(e)} \cdot \mathbf{j}_b^{(p)}) \quad (20)$$

with  $\mathbf{n}$  the normal pointing towards the inside of the capillary. Splitting the surface integrals between the ports and the tube walls, and using the boundary conditions (7), (10), (13), and (15), the above equality reads

$$\begin{aligned} & \int \int_{ports} \mathbf{n} \cdot (\boldsymbol{\sigma}^{(p)} \cdot \mathbf{v}^{(e)} - \phi^{(p)} \cdot \mathbf{j}_b^{(e)}) + \int \int_{walls} \mathbf{n} \cdot \boldsymbol{\sigma}^{(p)} \cdot (\mu \mathbf{E}^{(e)}) \\ &= \int \int_{ports} \mathbf{n} \cdot (\boldsymbol{\sigma}^{(e)} \cdot \mathbf{v}^{(p)} - \phi^{(e)} \cdot \mathbf{j}_b^{(p)}) \\ &+ \int \int_{walls} \phi^{(e)} (\nabla_s \cdot \mathbf{j}_s^{(p)}) \end{aligned} \quad (21)$$

then, as  $\mathbf{E}^{(e)}$  is tangent to the walls, the second term on the left-hand side of this equality can be rewritten:

$$\int \int_{walls} \mathbf{j}_s^{(p)} \cdot \mathbf{E}^{(e)} = - \int \int_{walls} \mathbf{j}_s^{(p)} \cdot \nabla_s \phi^{(e)} \quad (22)$$

so that one can rewrite the global equality as

$$\begin{aligned}
 & \int \int_{\text{ports}} \mathbf{n} \cdot (\boldsymbol{\sigma}^{(p)} \cdot \mathbf{v}^{(e)} - \phi^{(p)} \cdot \mathbf{j}_b^{(e)}) \\
 &= \int \int_{\text{ports}} \mathbf{n} \cdot (\boldsymbol{\sigma}^{(e)} \cdot \mathbf{v}^{(p)} - \phi^{(e)} \cdot \mathbf{j}_b^{(p)}) \\
 &+ \int \int_{\text{walls}} \nabla_s \cdot (\phi^{(e)} \mathbf{j}_s^{(p)}). \tag{23}
 \end{aligned}$$

Performing the integral over the walls, we arrive at

$$\begin{aligned}
 & \int \int_{\text{ports}} \mathbf{n} \cdot \boldsymbol{\sigma}^{(p)} \cdot \mathbf{v}^{(e)} - \int \int_{\text{ports}} \mathbf{n} \cdot (\phi^{(p)} \mathbf{j}_b^{(e)}) \\
 &= \int \int_{\text{ports}} \mathbf{n} \cdot \boldsymbol{\sigma}^{(e)} \cdot \mathbf{v}^{(p)} - \int \int_{\text{ports}} \mathbf{n} \cdot (\phi^{(e)} \cdot \mathbf{j}_b^{(p)}) \\
 &- \oint_{\text{portscontour}} \cdot (\phi^{(e)} \cdot \mathbf{j}_s^{(p)}) \tag{24}
 \end{aligned}$$

with  $\mathbf{n}_s$  the normal to the perimeter of the ports, along the walls, pointing inside the capillary. This is in general form the relation relating the generalized potentials at the borders of the capillary to the corresponding currents through the capillary.

If the inlets and outlets are smooth homogeneous capillaries (see Ref. [26] for a related discussion), then one can consider that on the ports the pressure  $p$  and the potential  $\phi$  are homogeneous across the section of the ports so that one can transform the previous equality into

$$(J_s^{(p)} + J_b^{(p)}) \cdot \Delta\Phi^{(e)} - J^{(e)} \cdot \Delta\Phi^{(p)} = Q^{(e)} \cdot \Delta P^{(p)} - Q^{(p)} \cdot \Delta P^{(e)}, \tag{25}$$

where  $\Delta P$  and  $\Delta\phi$  describe the pressure and potential increase from the inlet to the outlet in the two problems, and  $Q$  and  $J$  describe the flow rate and electric current running through the capillary. Note that as mentioned before the electric current through the ports has two contributions in the streaming problem,  $J^{(p)} = J_s^{(p)} + J_b^{(p)}$ .

The previous equations are equivalent to stating that the matrix that describes the linear response of the system is symmetric:

$$\begin{bmatrix} Q \\ J \end{bmatrix} = \begin{bmatrix} K & M \\ M & S \end{bmatrix} \begin{bmatrix} -\Delta P \\ -\Delta\Phi \end{bmatrix}. \tag{26}$$

which is the most usual form of the Onsager reciprocity relations. The symmetry of the matrix allows one to relate the outcome of various experiments, provided one pays attention to the quantities that are controlled. Namely this leads to the Saxon's relations:

$$\left( \frac{J^{(e)}}{\Delta P^{(e)}} \right)_{\Delta\Phi^{(e)}=0} = \left( \frac{Q^{(p)}}{\Delta\Phi^{(p)}} \right)_{\Delta P^{(p)}=0}, \tag{27}$$

$$\left( \frac{Q^{(e)}}{\Delta\Phi^{(e)}} \right)_{J^{(e)}=0} = - \left( \frac{J^{(p)}}{\Delta P^{(p)}} \right)_{Q^{(p)}=0}, \tag{28}$$

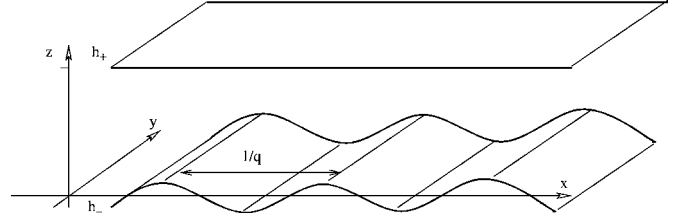


FIG. 5. Sketch of the channel. Upper and lower surfaces are respectively described by  $z=h_+(x,y)$  and  $z=h_-(x,y)$ , and bear a surface charge  $\sigma_+(x,y)$  and  $\sigma_-(x,y)$ .

$$\left( \frac{J^{(e)}}{Q^{(e)}} \right)_{\Delta\Phi^{(e)}=0} = - \left( \frac{\Delta P^{(p)}}{\Delta\Phi^{(p)}} \right)_{Q^{(p)}=0}, \tag{29}$$

$$\left( \frac{\Delta P^{(e)}}{J^{(e)}} \right)_{\Delta Q^{(e)}=0} = \left( \frac{\Delta\Phi^{(p)}}{Q^{(p)}} \right)_{J^{(p)}=0}. \tag{30}$$

Again we emphasize that these relations are valid beyond the approximations implicit in the present formalism, and thus not a new result. Nevertheless, the above calculation is a good consistency test, that also highlights the generic bulk+surface character of the streaming current pattern, a feature absent in the discussion of homogeneous flat geometries (see, e.g., Sec. II A). Some mechanisms for its generation will become clear in the next section when we consider specific patterned geometries.

#### IV. STRUCTURE OF THE ELECTROKINETICS FIELDS IN PATTERNED MICROFLUIDIC GEOMETRIES

In this section the analytical framework laid out in Sec. II is used to explicitly compute the electrokinetic fields (electric and hydrodynamic) generated by the application of pressure or potential drops in a few model patterned microfluidic geometries. The study of such model situations has already proven to be useful for electro-osmosis, as a way to understand how surface modifications and patterns can induce desired flow patterns [13,14,23], and as a way to quantify the resulting effects, e.g., for mixing, pumping, etc. As in previous papers [14,23] we consider patterns of topography and surface charged, used either separately or in a combined way. Here however, we will display results for streaming effects on an equal footing to those for electro-osmosis.

For the sake of simplicity, we focus on a rather slab geometry, with stripe patterns only, i.e., the surface charge or the topography are modulated along one direction only (see Fig. 5). To be more specific we consider two parallel plates, a distance  $H$  apart along the  $z$  direction. The surface properties are modulated along the  $x$  direction only. Our model for a modulation of the topography is that the locus of the top ( $h_+$ ) and bottom ( $h_-$ ) plates are

$$h_-(x,y) = \alpha H \cos(qx), \tag{31}$$

$$h_+(x,y) = H \tag{32}$$

with  $\mathbf{q} = q\mathbf{x}$  the modulation wave vector and  $\alpha$  a dimensionless measure of this topographic modulation. The surface

charge densities of both plates are assumed to be patterned in a symmetric way, in a manner described by a modulation of the *electroosmotic mobility* present in Eqs. (10) and (14):

$$\mu(x,y) = \bar{\mu} + \mu_0 \cos(qx + \theta) \quad (33)$$

with  $\bar{\mu}$  the average mobility and  $\mu_0$  a measure of the modulation.

Note that mathematically the status of the different modulations is different. The problem is linear in the  $\mu(x,y)$  so that one can for example analyze separately the problems for  $\mu_0=0$  and for  $\bar{\mu}=0$  and sum the resulting fields. On the contrary the problem is not linear in  $\alpha$ , and is treated perturbatively in this parameter.

Given this remark we focus in this section on the four following situations treated independently in four separate subsections:

Sec. IV A: a flat channel with homogeneous charge ( $\alpha=0, \bar{\mu} \neq 0, \mu_0=0$ ), as a reminder to set the stage;

Sec. IV B: a flat channel with a symmetric modulation of the surface charge ( $\alpha=0, \bar{\mu}=0, \mu_0 \neq 0$ );

Sec. IV C: a channel with a topographic modulation and a homogeneous charge ( $\alpha \neq 0, \bar{\mu} \neq 0, \mu_0=0$ ). The perturbative expansion is performed up to  $O(\alpha^2)$  terms;

Sec. IV D: a channel with both charge and topography modulations ( $\alpha \neq 0, \bar{\mu}=0, \mu_0 \neq 0$ ). The synergy between charge and topography modulation yields couplings at order  $O(\alpha)$ .

For each of these geometries, to fully describe the *linear response* considered here, it is necessary and sufficient to compute separately the electrokinetic response to pressure and electric fields applied along the modulation direction  $x$  (i.e., perpendicular to the stripes), and perpendicular to it along  $y$ . The response to any driving can then be obtained by a linear combination of the solutions presented here [23].

As this result in four cases per geometry, for the sake of readability of the text, the explicit (and sometimes lengthy) formulas for the resulting flow and current fields are given in a separate appendix for each of the four geometries (designed by the same letter A, B, C, or D), organized as follows. Each of these appendixes is split between a section I for driving fields applied along  $y$ , and a section II for fields applied along  $x$ . Each of these sections is split into three subsections: (a) describes results for electro-osmosis, (b) collects results for streaming currents, (c) summarizes in matrix form the net (average) electrokinetic response of the corresponding geometry to drivings in the corresponding direction. The results of the (c) subsections clearly show that for all the geometries these response matrices are symmetric as they should be [26]. We have also checked that the appropriate limits of these formulas coincide with published results obtained in the lubrication limit [23].

In the present main text we only comment on the most salient features of the results, analyzing on the physics at work. For these reasons we also focus essentially on the case of a driving along the modulation direction  $x$  (i.e., perpendicular to the stripes) when interesting local geometrical features can be observed. In contrast, due to the translational invariance of our model for patterned surfaces, drivings along the stripes yield only uniaxial, divergence free, electro-

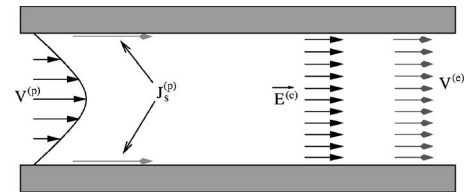


FIG. 6. Schematic representation of electrokinetic fields in a homogeneous straight channel. Left: a pressure drop induces a parabolic flow and surface streaming currents. Right: a potential drop induces a homogeneous current (and electric field) in the channel, and a pluglike electro-osmotic flow.

osmotic flows, or streaming currents. However, the fact that the global net response is anisotropic (i.e., different along  $x$  and  $y$ ) permits the generation and use of various transverse effects to be discussed in Sec. V.

### A. Reminder: A flat homogeneous channel

A schematic representation of the textbook results for the electrokinetic fields developing in this simple geometry is given in Fig. 6. The electro-osmotic flux is a pluglike flow and the streaming current is localized at the surface. The geometrical arrangements of the electro-osmotic and streaming current pattern are quite different. Yet the global response coefficients, when properly normalized, are equal in agreement with the necessary symmetry of the response matrix in Eq. (26).

### B. Flat channel with a symmetric modulation of the surface charge

On flat surfaces, when the surface charge is modulated, the electro-osmotic slip velocity is no more invariant and neither is the surface streaming current in the reciprocal situation. As a result, given the conservation laws for mass or charge, these surface heterogeneities result in flows or currents in the bulk of the channel as depicted in Fig. 7.

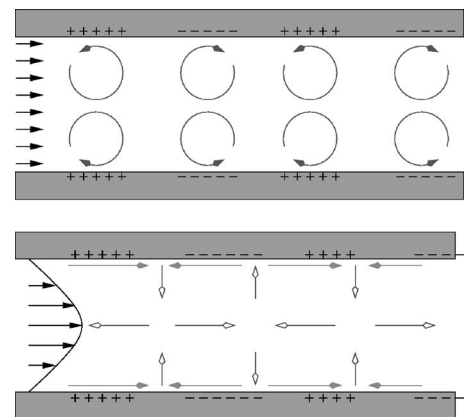


FIG. 7. Electro-osmotic flow (a) and streaming current pattern (b) developing in a straight channel with modulated charge surface when an electric field (a) or a pressure drop (b) is applied. The surface streaming currents  $J_s$  are symbolized by a filled arrow, and bulk streaming currents  $J_b$  by an empty arrow.

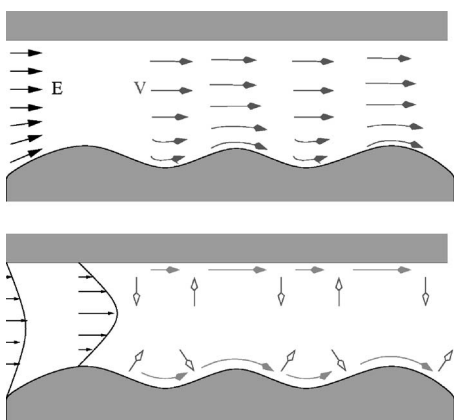


FIG. 8. Electro-osmotic flow (a) and streaming current (b) induced in an undulated homogeneous channel.

However, because of  $+/-$  symmetry in this system ( $\bar{\mu} = 0$ ), the net global electrokinetic coefficients of this model system are zero. In a generic system with nonzero  $\bar{\mu}$  and  $\mu_0$ , they would depend only on the former (one simply superimposes the results of this subsection to those of the previous one).

*Electro-osmotic flow.* The recirculation rolls induced by the modulated slip velocity have been predicted a decade ago and observed experimentally by Stroock *et al.* in microfluidic channel using neutral fluorescent beads [12]. Beyond allowing for the design of three-dimensional (3D) flows from 2D surface patterns, this effect is known to induce detrimental dispersion in electrophoresis experiments performed in heterogeneous channels.

*Streaming current.* As discussed in Sec. II, a modulation of the surface streaming current leads to current injection in the bulk in order to satisfy the charge conservation law. These recirculation structures are geometrically different from the ones obtained in the previous problem (electro-osmosis). Indeed the generated bulk streaming current is rotational free so that the recirculation structures are not *rolls* (no field lines closing on themselves in the bulk). The field lines originate and disappear in the surface which acts as a distribution of sources and sinks.

### C. Undulated channel with a homogeneous surface charge

In this geometry, deviations in the electro-osmotic flow and streaming current patterns occur at linear order in  $\alpha$ , but, as obvious from symmetry considerations, net electrokinetic couplings across the channel show up only at order  $\alpha^2$  (see Fig. 8).

*Electro-osmotic flow.* The surface charge being homogeneous, the electro-osmotic velocity field is at each point proportional to the electrical field, i.e.,  $\mathbf{v} = \mu\mathbf{E}$  everywhere. It thus follows the irrotational, divergence-free pattern of the electric field, with no salient features, increasing on the “hills” and decreasing in amplitude in the “valleys.”

*Streaming current.* In contrast there are interesting features showing up in the analysis of the streaming current pattern, even in the present case of homogeneously charged

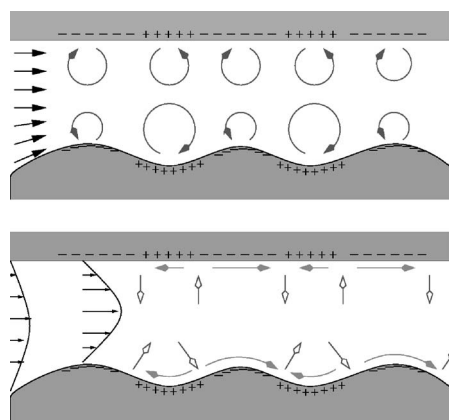


FIG. 9. Electro-osmotic flow (a) and streaming current (b) developing in an undulated charge-modulated channel. The present picture correspond to a specific offset between the charge and topography modulations.

surfaces, a point essentially absent in the electrokinetic literature.

Indeed, the pressure driven flow in such a channel is modulated along  $x$  because of the variations in thickness. This leads to a corresponding modulation of the shear (velocity gradients) on the bottom surface, with larger values on the hills. This directly translates into corresponding modulations of the surface streaming current, resulting in injection of bulk streaming currents as depicted in the figure. In agreement with this qualitative argument, the explicit calculations in Appendix C show that topography modulations generate bulk current structures, somewhat similarly to the surface charge modulations described in Sec. IV B.

### D. Undulated channel with a symmetric charge-density modulation

Adding a charge modulation to the previous picture lifts off symmetries present in the two previous cases. As a result net global electrokinetic effects are obtained at order  $\mu_0\alpha$ , with a sign that depends on the phase shift of the surface and topography modulations (i.e., are the negative charges on the hill or in the valleys?) [14,21] (see Fig. 9).

*Electro-osmotic flow.* As previously, slip velocity is greater at the restrictions but its direction changes periodically. Hydrodynamic recirculation rolls develop but with different amplitude and direction of rotation.

*Streaming current.* Direction and amplitude of surface streaming currents change periodically. Consequently a succession of current sources and drains is disposed along the surface. There is altogether a net streaming current in the channel, which travels across the channel using alternatively surface current or “leapfrog” trajectories between sources and sinks.

## V. DISCUSSION

We start this section with a rapid description of three directions of immediate application of our work.

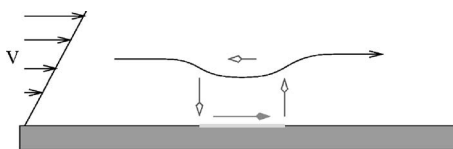


FIG. 10. Perturbation of the trajectory of a positively charged bead trajectory near a positively charged surface defect on an otherwise neutral surface. The surface streaming current recirculates in the bulk.

### A. Numerical analysis

Numerical analysis is widely used in microfluidics to anticipate the behavior of microsystems in order to avoid time-consuming prototyping. For example, simulations have shown the possibility to decrease electrophoretic longitudinal dispersion using a well chosen U shape [28]. Geometrical parameters of grooved channels have been numerically optimized to increase passive mixing [21]. Electro-osmotic and streaming current structures have been studied within shape and/or charge modulated channel especially by Li and co-workers [8,10,16,17].

The present work may be used in two directions for numerical analysis. First of all, analytical solutions can be used as benchmarks to test and validate numerical protocols in model geometries. Second, our analytical framework can be numerically implemented (e.g., in finite-element methods) to account simultaneously for streaming effects and electro-osmosis in complex geometries.

### B. Potential artefacts in particle image velocimetry

Highly accurate particle imagery velocimetry (PIV) is often required, for example, to quantify purely hydrodynamic slip [29,30]. Standard protocols use fluorescent beads that are charged to avoid flocculation. Those surface charges are usually supposed not to affect the measurement as long as no electrical field is applied, as is the case in standard measurement of “purely” hydrodynamic flows. Nonetheless, we have shown that hydrodynamic flows do generate not only surface streaming currents but also bulk streaming currents when surface charge or topography heterogeneities are present. The corresponding electrical field is then able to modify the bead trajectories even if they are not “on” the surface (Fig. 10).

The trajectory of the bead is perturbed by the induced streaming field which can lead to artefacts in velocity measurements close to the surface (i.e., a distance similar to the size of the defect  $w$ ). Let us provide here a rough estimate of the amplitude of this effect using a scaling analysis. Suppose the typical scale for the hydrodynamic velocity at a distance  $w$  of surface is  $v_{hydro}$ .

Using the equations of the second section, the shear rate of order  $v_{hydro}/w$ , leads to a surface streaming current on the defect,

$$J_s^{(p)} \sim -\epsilon \zeta_d \frac{v^{(p)}}{w} \sim \mu_d \eta \frac{v^{(p)}}{w}. \quad (34)$$

with  $\mu_d$  the surface electro-osmotic mobility of the defect. This current recirculates in the bulk of conductivity  $\gamma$  on a

region of volume  $\sim w^3$ , leading to a typical bulk electrical field

$$E^{(p)} \sim \frac{1}{\gamma} \frac{J_s^{(p)}}{w} \sim -\mu_d \eta \frac{v^{(p)}}{\gamma w^2}. \quad (35)$$

We may now estimate the electrophoretic velocity of the bead (electrophoretic mobility  $-\mu_b$ ) as

$$v^{(e)} \sim -\mu_b E^{(p)} \sim \frac{\mu_b \mu_d \eta}{\gamma w^2} v^{(p)}. \quad (36)$$

This measures the induced additional velocity due to the streaming effects induced by the surface defect. Taking as very reasonable values: size of the defect  $w=5 \mu\text{m}$ , electro-osmotic surface potential of the defect  $\zeta_d=25 \text{mV}$ , surface potential of the bead  $\zeta_b=25 \text{mV}$ , bulk conductivity  $\gamma = 1 \mu\text{S/m}$ , and viscosity  $\eta=10^{-3}$ , we obtain

$$v^{(e)} \approx v^{(p)} \quad (37)$$

showing that the perturbation can indeed be very substantial! This potentially large artefact is fundamentally related to the one discussed by Lauga [31] where the considered recirculation was at the scale of the capillary. In the present discussion the effect is enhanced by the localization close to the defect of the recirculating field lines.

### C. Transverse pumping efficiency prediction

Following an earlier theoretical analysis relying on a lubrication, a transverse electro-osmotic micropump was fabricated a couple of years ago and its ability to pump demonstrated and characterized [18]. It consisted in a channel bearing periodic grooves on one of its walls, disposed at an angle  $\pi/4$  with the channel axis. Two side electrodes are disposed on the lateral walls, and addressed with a 10-V potential difference, generating an electrical field perpendicular to the axis of the channel. The main features of the system are [18] 1 mm wide, 60  $\mu\text{m}$  high, modulation wavelength 140  $\mu\text{m}$ , modulation amplitude  $\alpha=0.16$ , electro-osmotic mobility  $\mu=6 \mu\text{m s}^{-1} (\text{V/cm})^{-1}$ .

The electrical field imposed by the electrodes induces a transverse electro-osmotic flow with a contribution along the main direction of the channel  $x$ . Its average velocity  $v_x$  can be estimated within our analytical framework (see Appendix C), with the additional approximation of describing the square shaped grooves by the sinusoid used in our calculations. We find

$$v_x \approx 10 \mu\text{m s}^{-1}. \quad (38)$$

But the induced electroosmotic flow has also a contribution perpendicular to the channel. This contribution generates a pressure drop between the lateral wall and consequently a hydrodynamic flow which also has a contribution along  $x$ . We find it with our formula to be in the opposite direction to the direct transverse electro-osmotic effect. The corresponding average velocity  $v_x'$  is given by

$$v_x' \approx -60 \mu\text{m s}^{-1}. \quad (39)$$

Thus our analytical calculations help here in two ways. First they point out that the net pumping effect is opposite to the

direct “transverse electro-osmosis” (which is far from obvious at first sight). Second they provide an estimate for the pumping velocity of  $\sim -50 \mu\text{m s}^{-1}$ . Both are consistent with the measured values of  $\sim -80 \mu\text{m s}^{-1}$  [18] (the difference in the exact numbers is very reasonable given the differences between the precise experimental geometry—square-shaped grooves—and the sinusoids used for the perturbative theoretical calculation).

This example demonstrates the interest of such a computational method for the assessment of microfluidic functions. We recall that the complete framework presented here underlines that the same device can be used as an integrated flowmeter if the electrodes are used to measure streaming currents or potential. The reciprocal relations demonstrated in Sec. III may also be used to predict the electro-osmotic pumping efficiency from a streaming current measurement.

#### D. Conclusion

In conclusion, we have provided an operational analytical framework to describe electrokinetic effects in arbitrary geometries, valid provided the surface potential is moderate and the electrical double layer is thin. Although this recipe has been widely used for electro-osmotic flows, such is not the case for the description of streaming potential and currents. We have pointed out that topographic or charge-density surface heterogeneities will likely generate streaming currents in the bulk under pressure driven flows. Altogether this balanced consistent description allows one to investigate analytically the effect of patterns in microfluidic geometries and an evaluation of the resulting functionalities.

#### ACKNOWLEDGMENTS

A.A. thanks the French Ministère de la Recherche for an ACI grant.

#### APPENDIX A: RESULTS FOR A FLAT HOMOGENEOUS CHANNEL

We provide here the explicit results for Sec. IV A and consider a flat homogeneous channel, for which the results are simple and well known (Fig. 6), and furthermore do not depend on the direction along which fields are applied given the symmetry of the problem. We present them explicitly mostly as they serve as the zeroth-order solution for shape modulations considered in Appendix C.

##### 1. Electro-osmosis

An applied potential drop (e.g., along  $x$ ) results in a uniform electrical field in the channel:

$$\mathbf{E}^{(e)} = -\frac{\Delta\Phi}{L}\mathbf{x} \quad (\text{A1})$$

which generates a uniform electro-osmotic flow:

$$\mathbf{v}^{(e)}(x, y, z) = -\mu\frac{\Delta\Phi}{L}\mathbf{x}. \quad (\text{A2})$$

##### 2. Streaming current

An applied pressure drop (e.g., along  $x$ ) generates the classical parabolic flow profile:

$$\mathbf{v}^{(p)} = \frac{1}{2\eta}z(H-z)\left(-\frac{\Delta P}{L}\right)\mathbf{x} \quad (\text{A3})$$

which induces surface streaming currents:

$$\mathbf{j}^{(p)} = -\mu H/2\left(-\frac{\Delta P}{L}\right)\mathbf{x}. \quad (\text{A4})$$

##### 3. Net linear response

Along any direction the total electrical current  $J$  and hydrodynamic flow  $Q$  are related to the applied fields by

$$\begin{bmatrix} Q \\ J \end{bmatrix} = \begin{bmatrix} \frac{H^3}{12\eta} & -\mu H \\ -\mu H & \gamma_{el}H \end{bmatrix} \begin{bmatrix} \left(-\frac{\Delta P}{L}\right) \\ \left(-\frac{\Delta\phi}{L}\right) \end{bmatrix}. \quad (\text{A5})$$

#### APPENDIX B: RESULTS FOR A FLAT CHANNEL BEARING A SINUSOIDAL CHARGE VARIATION

We provide here the explicit results for Section IV B and consider a flat channel with a modulated surface charge so that its electro-osmotic mobility is on both plates  $\mu_{\pm} = \mu_{\pm} \cos(qx)$ . The average mobility is taken zero for simplicity, as this would simply lead to adding solutions of Appendix A. The driving electric field and pressure field are uniform in all the situations below.

##### 1. Applied field along $y$ , perpendicular to the modulation

###### a. Electro-osmosis

An imposed electric field  $-\frac{\Delta\Phi}{L}$  along  $y$  generates a velocity field along the same direction:

$$\mathbf{v}^{(e)} = -\mu_0 \frac{\cosh[q(z-H/2)]}{\cosh(qH/2)} \cos(qx) \left(-\frac{\Delta\Phi}{L_y}\right)\mathbf{y}. \quad (\text{B1})$$

Given its simple Laplacian structure, the flow generated by the modulation decays exponentially away from the wall over the typical length  $1/q$ .

###### b. Streaming current

A pressure drop along  $y$  generates a streaming current in the same direction, of amplitude modulated along  $x$ . This ensures a surface-divergence-free situation with the streaming currents confined to the surface:

$$\mathbf{j}_s^{(p)} = -\frac{\mu_0 H}{2} \cos(qx) \left(-\frac{\Delta P}{L_y}\right)\mathbf{y}. \quad (\text{B2})$$

###### c. Net linear response

Integrating along  $z$  is not sufficient to yield equality of the response coefficient for the two effects:

$$J^{(p)} = -\mu_0 H \cos(qx) \left( -\frac{\Delta P}{L} \right), \quad (\text{B3})$$

$$Q^{(e)} = -\mu_0 \frac{2 \sinh(qH/2)}{q \cosh(qH/2)} \cos(qx) \left( -\frac{\Delta \Phi}{L} \right). \quad (\text{B4})$$

However, averaging over a period of the modulation does yield back a trivially symmetric matrix for the global response, with zero diagonal coefficients given the  $+/-$  symmetry of the problem,

$$\begin{bmatrix} \langle Q_y \rangle \\ \langle J_y \rangle \end{bmatrix} = \begin{bmatrix} \frac{H^3}{12\eta} & 0 \\ 0 & \gamma_{el} H \end{bmatrix} \begin{bmatrix} -\nabla P_y \\ -\nabla \Phi_y \end{bmatrix}. \quad (\text{B5})$$

## 2. Applied field along $x$ , parallel to the modulation

### a. Electro-osmosis

This geometry yields recirculation rolls with induced local pressure gradients as already described in Ref. [13] (Fig. 7). The corresponding stream function is given by:

$$\begin{aligned} \psi_v^{(e)} = & -\mu_0 \frac{\frac{H}{2} \cos\left(\frac{qH}{2}\right) \sinh(q \cdot u) - u \sinh\left(\frac{qH}{2}\right) \cosh(q \cdot u)}{\frac{qH}{2} - \sinh\left(\frac{qH}{2}\right) \cosh\left(\frac{qH}{2}\right)} \\ & \times \cos(qx + \theta) \left( -\frac{\Delta \Phi}{L} \right) \end{aligned} \quad (\text{B6})$$

with  $u = z - \frac{H}{2}$ . The velocity field is then simply given by  $\mathbf{v}^{(e)} \cdot \mathbf{x} = \frac{\partial \psi_v^{(e)}}{\partial z}$  and  $\mathbf{v}^{(e)} \cdot \mathbf{z} = -\frac{\partial \psi_v^{(e)}}{\partial x}$ .

### b. Streaming current

The surface streaming current now varies along the surface

$$\mathbf{j}_{surf}^{(p)} = -\mu_0 H \cos(qx) \left( -\frac{\Delta P}{L_x} \right) \quad (\text{B7})$$

generating bulk streaming currents schematically represented in Fig. 7. The corresponding electrical “streaming potential” is

$$\phi^{(p)} = -\mu_0 H \frac{\cosh\left[q\left(\frac{H}{2} - z\right)\right]}{\sinh\left(\frac{qH}{2}\right)} \sin(qx + \theta) \left( -\frac{\Delta P}{L_x} \right) \quad (\text{B8})$$

wherefrom one derives the bulk streaming current using Ohm’s law  $\mathbf{j}_b^{(p)} = -\gamma_{el} \nabla \phi^{(p)}$  with  $\gamma_{el}$  the electrical conductivity.

### c. Net linear response

Integration along  $z$  and  $x$  again yields a trivially symmetric matrix:

$$\begin{bmatrix} \langle Q_x \rangle \\ \langle J_x \rangle \end{bmatrix} = \begin{bmatrix} \frac{H^3}{12\eta} & 0 \\ 0 & \gamma_{el} H \end{bmatrix} \begin{bmatrix} \left( -\frac{\Delta P}{L} \right) \\ \left( -\frac{\Delta \Phi}{L} \right) \end{bmatrix}. \quad (\text{B9})$$

## APPENDIX C: RESULTS FOR A HOMOGENEOUSLY CHARGED CHANNEL WITH A TOPOGRAPHIC MODULATION

We provide here the explicit results for Sec. IV C and consider a channel with a constant electro-osmotic mobility  $\bar{\mu}$ , and a modulation of its bottom surface  $h_-(x, y) = \alpha H \cos(qx)$ . Hydrodynamics in this geometry has been previously investigated by Stroock *et al.* who characterize transverse flow generation for various microfluidic applications [22].

### 1. Applied field along $y$ , perpendicular to the modulation

#### a. Electro-osmosis

The applied electrical field is in this geometry uniform  $\mathbf{E}^{(e)} = \left( -\frac{\Delta \Phi}{L_y} \right) \mathbf{y}$ , and so is electro-osmosis:

$$\mathbf{v}^{(e)} = \bar{\mu} \left( -\frac{\Delta \Phi}{L_y} \right) \mathbf{y}. \quad (\text{C1})$$

#### b. Streaming current

The velocity field generated by a pressure drop along  $y$  is to second order in  $\alpha$  [32]:

$$\mathbf{v}^{(p)} = \frac{H^2}{2\eta} \left[ \frac{z(H-z)}{H^2} - \frac{1}{2} \alpha^2 K_{\perp}(qH) \frac{H-z}{H} + T_{\perp}(x, z) \right] \left( -\frac{\Delta P}{L_y} \right) \mathbf{y} \quad (\text{C2})$$

with  $T_{\perp}(x, z)$  corresponding to periodic rolls structures of zero average along  $x$ . Formulas for  $T_{\perp}(x, z)$  and  $K_{\perp}(qH)$  are provided in Appendix E.

From this we can compute the shear rate on the walls and thus the surface streaming currents. We obtain for the bottom wall

$$\begin{aligned} \mathbf{j}_{s-}^{(p)} = & -\frac{\bar{\mu} H}{2} \left[ 1 + \alpha \left( -2 + qH \frac{\cosh(qH)}{\sinh(qH)} \right) \cos(qx) \right. \\ & \left. + \alpha^2 \left( \frac{1}{2} K_{\perp}(qH) - \frac{1}{4} (qH)^2 - L_{\perp}(2qH) \cos(2qx) \right) \right] \\ & \times \left( -\frac{\Delta P}{L_y} \right) \end{aligned} \quad (\text{C3})$$

with  $L_{\perp}$  given in Appendix E, and for the top wall

$$\begin{aligned} \mathbf{j}_{s+}^{(p)} = & -\frac{\bar{\mu} H}{2} \left[ 1 - \alpha \frac{qH}{\sinh(qH)} \cos(qx) + \alpha^2 \left( -\frac{1}{2} K_{\perp}(qH) \right. \right. \\ & \left. \left. - \frac{qH}{\sinh(2qH)} \cos(2qx) \right) \right] \left( -\frac{\Delta P}{L_y} \right). \end{aligned}$$

Summing these expressions along  $x$  allows us to calculate the average streaming current per unit length:

$$\langle J_s^{(p)} \rangle = -\mu H \left( -\frac{\Delta P}{L_y} \right). \quad (C4)$$

### c. Net linear response

The response matrix  $M_y$  is then

$$\begin{bmatrix} \frac{H^3}{12\eta} & -\mu H \\ -\mu H & \gamma_{el} H \end{bmatrix}. \quad (C5)$$

## 2. Applied field along $x$ , parallel to the modulation

### a. Electro-osmosis

Solving Laplace equation, we find to second order in  $\alpha$  the pattern of the driving electric field:

$$\begin{aligned} (-\nabla \phi_x^{(e)}) &= \left( 1 + \alpha q H \frac{\cosh[q(H-z)]}{\sinh(qH)} \cos(qx) \right. \\ &\quad \left. + \alpha^2 (qH)^2 \frac{\cosh(qH)}{\sinh(qH)} \frac{\cosh[2q(H-z)]}{\sinh(2qH)} \cos(2qx) \right) \\ &\quad \times (-\nabla \Phi_x), \end{aligned}$$

$$\begin{aligned} (-\nabla \phi_z^{(e)}) &= \left( 0 - \alpha q H \frac{\sinh[q(H-z)]}{\sinh(qH)} \sin(qx) \right. \\ &\quad \left. - \alpha^2 (qH)^2 \frac{\cosh(qH)}{\sinh(qH)} \frac{\sinh[2q(H-z)]}{\sinh(2qH)} \sin(2qx) \right) \\ &\quad \times (-\nabla \Phi_x). \end{aligned}$$

The total electrical current is given by

$$J_x^{(e)} = H \left( 1 - \frac{1}{2} \alpha^2 q H \frac{\cosh(qH)}{\sinh(qH)} \right) \left( -\frac{\Delta \phi}{L_x} \right). \quad (C6)$$

As the electro-osmotic mobility is uniform, electro-osmosis is everywhere proportional to electrical field:

$$\mathbf{v}^{(e)} = -\bar{\mu} (-\nabla \phi^{(e)}). \quad (C7)$$

The electro-osmosis flow (per unit length in the  $y$  direction) integrated along  $z$  is a conserved quantity,

$$Q^{(e)} = -\bar{\mu} H \left( 1 - \frac{1}{2} \alpha^2 q H \frac{\cosh(qH)}{\sinh(qH)} \right) \left( -\frac{\Delta \Phi}{L_x} \right). \quad (C8)$$

### b. Streaming current

The velocity field induced by a pressure drop along  $x$  is a parabolic profile plus nonzeroth-order recirculation rolls [32]. Its structure is given by

$$\begin{aligned} \mathbf{v}_x^{(p)} &= \frac{H^2}{2\eta} \left( \frac{z(H-z)}{H^2} - \frac{1}{2} \alpha^2 K_{\parallel}(qH) \frac{H-z}{H} - \alpha \frac{dg_q}{dz}(z) \cos(qx) \right. \\ &\quad \left. + \frac{1}{2} \alpha^2 \frac{dh_q}{dz}(z) \cos(2qx) \right) \left( -\frac{\Delta P}{L_x} \right), \end{aligned}$$

$$\mathbf{v}_z^{(p)} = \frac{H^2}{2\eta} \left[ -\alpha g_q(z) \sin(qx) + \alpha^2 h_q(z) \sin(2qx) \right] \left( -\frac{\Delta P}{L_x} \right)$$

with  $g_q(z)$  and  $h_q(z)$  given in Appendix E.

Integrating along  $z$  yields the conserved flow rate

$$Q^{(p)} = \frac{H^3}{12\eta} \left( 1 + \frac{3}{2} \alpha^2 [1 - K_{\parallel}(qH)] \right) \left( -\frac{\Delta P}{L} \right). \quad (C9)$$

The induced surface streaming currents are given in the surface referential by

$$\begin{aligned} j_{surf}^{(p)}(H) &= \mu_0 \frac{H}{2} \left( -1 - \alpha H \ddot{g}_q(H) \cos(qx) + \frac{1}{2} \alpha^2 [K_{\parallel}(qH) \right. \\ &\quad \left. + H \ddot{h}_q(H) \cos(2qx)] \right) \left( -\frac{\Delta P}{L_x} \right), \end{aligned}$$

$$\begin{aligned} j_{surf}^{(p)}(z_-) &= \mu_0 \frac{H}{2} \left\{ -1 + \alpha [2 + H \ddot{g}_q(0)] \cos(qx) - \frac{1}{2} \alpha^2 \left[ K_{\parallel}(qH) \right. \right. \\ &\quad \left. - H \ddot{g}_q(0) + \frac{3}{2} (qH)^2 + \left( H^2 \ddot{g}_q(0) + \frac{3}{2} (qH)^2 \right. \right. \\ &\quad \left. \left. - H \ddot{h}_q(0) \right) \cos(2qx) \right\} \left( -\frac{\Delta P}{L_x} \right). \end{aligned}$$

Their sum averaged along  $x$  over a period is

$$J_s = -\mu_0 H \left[ 1 - \frac{1}{2} \alpha^2 (qH)^2 \frac{\sinh^2(qH)}{\sinh^2(qH) - (qH)^2} \right] \left( -\frac{\Delta P}{L_x} \right). \quad (C10)$$

As the surface streaming currents are not divergence free, there is charge injection into the bulk resulting in bulk streaming currents. These can be obtained using Ohm's law and the following electrostatic (streaming) potential:

$$\begin{aligned} \phi_b^{(p)}(x, z) &= \mu_0 \frac{H}{2} \left\{ \alpha \left( H \ddot{g}_q(H) \frac{\cosh(qz)}{\sinh(qH)} - [2 \right. \right. \\ &\quad \left. \left. + H \ddot{g}_q(0)] \frac{\cosh[q(H-z)]}{\sinh(qH)} \right) \sin(2qx) - \frac{\alpha^2}{2} \left[ [2 \right. \right. \\ &\quad \left. \left. + H \ddot{g}_q(0)] q^2 H \frac{\sinh[2q(H-z)]}{\sinh(2qH)} + \left( H^2 \ddot{g}_q(0) \right. \right. \\ &\quad \left. \left. + \frac{3}{2} (qH)^2 - H \ddot{h}_q(0) \right) \frac{\cosh[2q(H-z)]}{\sinh(2qH)} \right] \sin(2qx) \right\} \\ &\quad \times \left( -\frac{\Delta P}{L_x} \right). \end{aligned}$$

The average contribution of these bulk currents over a period is

$$\begin{aligned} J_b &= \bar{\mu} \frac{H}{2} \alpha^2 \left[ qH \frac{\cosh(qH)}{\sinh(qH)} - (qH)^2 \frac{\sinh^2(qh)}{\sinh^2(qH) - (qH)^2} \right] \\ &\quad \times \left( -\frac{\Delta P}{L_x} \right). \quad (C11) \end{aligned}$$

Summing up the surface and bulk contributions, we obtain the total streaming current along the channel:

$$J_x = -\bar{\mu}H \left[ 1 - \frac{1}{2}\alpha^2 qH \frac{\cosh(qH)}{\sinh(qH)} \right] \left( -\frac{\Delta P}{L_x} \right), \quad (\text{C12})$$

which is indeed constant along  $x$ , so as to respect charge conservation. Periodic surface and bulk contributions cancel out (Fig. 8).

### c. Net linear response

The  $M_x$  conductance matrix is then symmetric given by

$$M_x = \begin{bmatrix} \frac{H^3}{12\eta} \left\{ 1 + \frac{3}{2}\alpha^2 [1 - K_{||}(qH)] \right\} & -\bar{\mu}H \left( 1 - \frac{1}{2}\alpha^2 qH \frac{\cosh(qH)}{\sinh(qH)} \right) \\ -\bar{\mu}H \left( 1 - \frac{1}{2}\alpha^2 qH \frac{\cosh(qH)}{\sinh(qH)} \right) & \gamma_{el}H \left( 1 - \frac{1}{2}\alpha^2 qH \frac{\cosh(qH)}{\sinh(qH)} \right) \end{bmatrix}. \quad (\text{C13})$$

### 3. Global response of a homogeneous undulated channel

Putting together all the above results, the global response of the channel to fields applied in arbitrary directions is described by:

$$\begin{bmatrix} Q_x \\ J_x \\ \langle Q_y \rangle \\ \langle J_y \rangle \end{bmatrix} \begin{bmatrix} M_x & 0 \\ 0 & M_y \end{bmatrix} \begin{bmatrix} \left( -\frac{\Delta P}{L_x} \right) \\ \left( -\frac{\Delta \phi}{L_x} \right) \\ \left( -\frac{\Delta P}{L_y} \right) \\ \left( -\frac{\Delta \phi}{L_y} \right) \end{bmatrix}, \quad (\text{C14})$$

with  $M_y$  and  $M_x$  defined above [Eqs. (C5) and (C13)].

In the limit where the lubrication approximation holds, i.e.,  $qH \ll 1$ , we recover the results derived directly by Ajdari [23]:

$$M_{\text{lubri}} = \begin{bmatrix} \frac{H^3}{12\eta} (1 - 3\alpha^2) & -\bar{\mu}H \left( 1 - \frac{1}{2}\alpha^2 \right) & 0 & 0 \\ -\bar{\mu}H \left( 1 - \frac{1}{2}\alpha^2 \right) & \gamma_{el}H \left( 1 - \frac{1}{2}\alpha^2 \right) & 0 & 0 \\ 0 & 0 & \frac{H^3}{12\eta} \left( 1 + \frac{3}{2}\alpha^2 \right) & -\bar{\mu}H \\ 0 & 0 & -\bar{\mu}H & \gamma_{el}H \end{bmatrix}. \quad (\text{C15})$$

This asymptotic formulas make it clear that the electrokinetic response coefficients are different along  $x$  and  $y$ , so that applied fields at some angle with the symmetry axis of the channel will generate transverse effects, i.e., perpendicular to the field that generates them.

This holds clearly true beyond the lubrication approximation. Such transverse effects are of order  $\alpha^2$  in the present perturbation scheme, which is, however, likely to permit an estimation of their amplitude (this worked rather well for the purely hydrodynamic response, see Ref. [32]). We use it here in particular to estimate the expected pumping by transverse

electroosmotic flow in the device of Gitlin *et al.* [18] as discussed in Sec. V C.

### APPENDIX D: RESULTS FOR A CHANNEL WITH MODULATIONS OF TOPOGRAPHY AND SURFACE CHARGE

We provide here the explicit results for Sec. IV C and consider a channel with a modulation of its electro-osmotic mobility  $\mu_{\pm} = \mu_{\pm} \cos(qx)$ , and a modulation of its bottom surface  $h_{\pm}(x, y) = \alpha H \cos(qx)$ .

As described in Refs. [13,14,23], the coupling of both modulations yields here transverse electrokinetic effects that are first order in  $\alpha$  and proportional to  $\mu_0$ , so that we will limit our computations to that order.

## 1. Applied field along y, perpendicular to the modulation

### a. Electro-osmosis

The electro-osmotic velocity field is given by

$$v^{(e)} = -\mu_0 \left[ \frac{\cosh[q(z-H/2)]}{\cosh(qH/2)} \cos(qx + \theta) + \frac{\alpha}{2} qH \frac{\sinh(qH/2)}{\cosh(qH/2)} \left( \frac{H-z}{H} \cos(\theta) + \frac{\sinh[2q(z-H)]}{\sinh(2qH)} \cos(2qx + \theta) \right) \right] \left( -\frac{\Delta\Phi^{(e)}}{L_y} \right). \quad (D1)$$

The corresponding electro-osmotic flow rate is

$$M_y = \left[ \begin{array}{c} \frac{H^3}{12\eta} \left\{ 1 + \frac{3}{2} \alpha^2 [1 - K_\perp(qH)] \right\} \\ -\mu H \cos \theta \alpha \left( 1 - \frac{qH \sinh(qH/2)}{2 \cosh(qH/2)} \right) \\ \gamma_e H \end{array} \right] \left( -\frac{\Delta\Phi^{(e)}}{L_y} \right). \quad (D5)$$

## 2. Applied field along x, parallel to the modulation

### a. Electro-osmosis

The electro-osmosis velocity field is (Fig. 9)

$$v_x^{(e)} = -\mu_0 \left[ \frac{\cosh[q(z-H/2)]}{\cosh(qH/2)} \cos(qx + \theta) + \frac{\alpha}{2} qH \frac{\sinh(qH/2)}{\cosh(qH/2)} \left( \frac{H-z}{H} \cos(\theta) + \frac{\sinh[2q(z-H)]}{\sinh(2qH)} \cos(2qx + \theta) \right) \right] \left( -\frac{\Delta\Phi^{(e)}}{L_y} \right) \quad (D6)$$

and the flow

$$Q_x^{(e)} = -\mu_0 H \frac{\alpha}{2} \left( -1 + \frac{1}{2} \frac{qH[1 + \cosh(qH)]}{\sinh(qH)} - qH \frac{\cosh(qH) - 1}{qH - \sinh(qH)} \right) \cos(\theta) \left( -\frac{\Delta\Phi^{(e)}}{L_y} \right). \quad (D7)$$

$$Q^{(e)} = -\mu_0 H \frac{\alpha}{2} \cos(\theta) \left( 1 - \frac{qH \sinh(qH/2)}{2 \cosh(qH/2)} \right) \left( -\frac{\Delta\Phi^{(e)}}{L_y} \right). \quad (D2)$$

### b. Streaming current

The streaming current is described by

$$J_s^{(p)} = -\mu_0 H \times \left[ \cos(qx + \theta) - \frac{\alpha}{2} \left( 1 - \frac{qH \sinh(qH/2)}{2 \cosh(qH/2)} \right) [\cos(\theta) + \cos(2qx + \theta)] \right] \left( -\frac{\Delta P^{(p)}}{L_y} \right), \quad (D3)$$

the average of which is

$$J_s^{(p)} = -\mu_0 H \frac{\alpha}{2} \cos(\theta) \left( -1 + \frac{qH \sinh(qH/2)}{2 \cosh(qH/2)} \right) (-\nabla P_y^{(p)}). \quad (D4)$$

### c. Net linear response

Relations between averaged fluxes and applied fields are

$$- \mu H \cos \theta \alpha \left( 1 - \frac{qH \sinh(qH/2)}{2 \cosh(qH/2)} \right) \left[ \begin{array}{c} \\ \gamma_e H \end{array} \right]. \quad (D5)$$

### b. Streaming current

Surface streaming currents on the lower plate  $\mathbf{j}_{surf}^{(p)}(z_-)$  and the upper plate  $\mathbf{j}_{surf}^{(p)}(H)$  are, respectively,

$$\mathbf{j}_{surf}^{(p)}(H) = -\mu_0 \frac{H}{2} \times \left[ \cos(qx + \theta) + \alpha qH \frac{qH \cosh(qH) - \sinh(qH)}{\sinh^2(qH) - (qH)^2} [\cos \theta + \cos(2qx + \theta)] \right] \left( -\frac{\Delta P}{L} \right),$$

$$\mathbf{j}_{surf}^{(p)}(z_-) = -\mu_0 \frac{H}{2} \left[ \cos(qx + \theta) + \frac{\alpha}{2} \left( qH \frac{\sinh(2qH) - 2qH}{\sinh^2(qH) - (qH)^2} - 2 \right) [\cos \theta + \cos(2qx + \theta)] \right] \left( -\frac{\Delta P}{L} \right)$$

which vary in space so that there is generation of bulk streaming currents (Fig. 9). The averaged surface current is

$$J_{surf} = -\mu_0 H \frac{\alpha}{2} \cos \theta \left[ -1 - qH \frac{1 - \cosh(qH)}{\sinh(qH) - qH} \right] \left( -\frac{\Delta P}{L_x} \right),$$

$$J_b = -\mu_0 H \frac{\alpha}{2} \cos \theta \left[ -\frac{1}{2} qH \frac{1 + \cosh(qH)}{\sinh(qH)} \right] \left( -\frac{\Delta P}{L_x} \right). \quad (D8)$$

Once again the periodic terms in the surface and bulk streaming currents cancel out, so as to ensure charge conservation and thus a constant overall streaming current along the channel.

### c. Synthesis

The corresponding response matrix  $M_x$  is

$$M_x = \begin{bmatrix} \frac{H^3}{12\eta} \left[ 1 + \frac{3}{2} \alpha^2 (1 - K_{\parallel}(qH)) \right] & -\mu_0 H \frac{\alpha}{2} \cos \theta \left( -1 + \frac{qH}{2} \frac{1 + \cosh(qH)}{\sinh(qH)} \right) \\ -\mu_0 H \frac{\alpha}{2} \left( -1 + \frac{qH}{2} \frac{1 + \cosh(qH)}{\sinh(qH)} \right) & \gamma_{el} H \left( 1 - \frac{1}{2} \alpha^2 qH \frac{\cosh(qH)}{\sinh(qH)} \right) \end{bmatrix}. \quad (D9)$$

### 3. Conclusion for an undulated heterogeneous channel

Putting together all these results leads to the following general symmetric response matrix:

$$\begin{bmatrix} Q_x \\ J_x \\ \langle Q_y \rangle \\ \langle J_y \rangle \end{bmatrix} \begin{bmatrix} M_x & 0 \\ 0 & M_y \end{bmatrix} \begin{bmatrix} \left( -\frac{\Delta P}{L_x} \right) \\ \left( -\frac{\Delta \phi}{L_x} \right) \\ \left( -\frac{\Delta P}{L_y} \right) \\ \left( -\frac{\Delta \phi}{L_y} \right) \end{bmatrix}, \quad (D10)$$

with  $M_x$  and  $M_y$  [Eqs. (D9) and (D5)].

### APPENDIX E: FORMULAS FOR SPECIAL FUNCTIONS

$$T_{\perp}(x, z) = -\alpha \frac{\sinh[q(h-z)]}{\sinh(qH)} \cos(qx) - \frac{1}{2} \alpha^2 K_{\perp}(qh) \frac{\sinh[2q(h-z)]}{\sinh(2qH)} \cos(2qx), \quad (E1)$$

$$K_{\perp}(u) = -1 + u \frac{\cosh(u)}{\sinh(u)}, \quad (E2)$$

$$L_{\perp}(u) = \frac{u}{2} \left( \frac{u}{4} - \frac{\cosh(u)}{\sinh(u)} \right), \quad (E3)$$

$$K_{\parallel}(u) = -1 + 2u \frac{\sinh(u) \cosh(u) - u}{\sinh^2(u) - u^2}, \quad (E4)$$

$$g_q(z) = \frac{\sinh(qH)z \sinh[q(H-z)] - qH(H-z) \sinh(qz)}{\sinh(qH)^2 - (qH)^2}, \quad (E5)$$

$$\ddot{g}_q(0) = 2q \frac{-\sinh(qH) \cosh(qH) + qH}{\sinh(qH)^2 - (qH)^2}, \quad (E6)$$

$$\ddot{g}_q(H) = 2q \frac{-\sinh(qH) + qH \cosh(qH)}{\sinh(qH)^2 - (qH)^2}, \quad (E7)$$

$$\ddot{\ddot{g}}_q(0) = q^2 \frac{3 \sinh(qH)^2 - (qH)^2}{\sinh(qH)^2 - (qH)^2}, \quad (E8)$$

$$\ddot{\ddot{g}}_q(H) = q^2 \frac{3qH \sinh(qH) - qH \cosh(qH) \sinh(qH)}{\sinh(qH)^2 - (qH)^2}. \quad (E9)$$

- [1] H. J. Crabtree, E. C. S. Cheong, D. A. Tilroe, and C. J. Backhouse, *Anal. Chem.* **73**, 4079 (2001).  
 [2] X. Ren, M. Bachman, C. Sims, G. P. Li, and N. Allbritton, *J. Chromatogr., B: Biomed. Appl.* **762**, 117 (2001).

- [3] J. Gaudioso and H. G. Craighead, *J. Chromatogr., A* **971**, 249 (2002).  
 [4] G. J. Fiechner and E. B. Cummings, *Anal. Chem.* **75**, 4747 (2003).

- [5] H. A. Stone, A. D. Stroock, and A. Ajdari, *Annu. Rev. Fluid Mech.* **36**, 381 (2004).
- [6] R. R. Netz, *Phys. Rev. E* **60**, 3174 (1999).
- [7] L. Joly, C. Ybert, E. Trizac, and L. Bocquet, *Phys. Rev. Lett.* **93**, 257805 (2004).
- [8] Y. Hu, C. Werner, and D. Li, *Anal. Chem.* **75**, 5747 (2003).
- [9] D. Sinton and D. Li, *Colloids Surf., A* **222**, 273 (2003).
- [10] D. Erickson and D. Li, *Langmuir* **18**, 1883 (2002).
- [11] D. Erickson and D. Li, *J. Colloid Interface Sci.* **237**, 283 (2001).
- [12] A. D. Stroock, M. Weck, D. T. Chiu, W. T. S. Huck, P. J. A. Kenis, R. F. Ismagilov, and G. M. Whitesides, *Phys. Rev. Lett.* **84**, 3314 (2000).
- [13] A. Ajdari, *Phys. Rev. Lett.* **75**, 755 (1995).
- [14] A. Ajdari, *Phys. Rev. E* **53**, 4996 (1996).
- [15] L. Ren and D. Li, *J. Colloid Interface Sci.* **243**, 255 (2001).
- [16] D. Erickson and D. Li, *Langmuir* **18**, 8949 (2002).
- [17] E. Biddiss, D. Erickson, and D. Li, *Anal. Chem.* **76**, 3208 (2004).
- [18] I. Gitlin, A. D. Stroock, G. M. Whitesides, and A. Ajdari, *Appl. Phys. Lett.* **83**, 1486 (2003).
- [19] D. Burgreen and F. R. Nakache, *J. Phys. Chem.* **68**, 1084 (1964).
- [20] L.-M. Fu, R.-J. Yang, and G.-B. Lee, *Anal. Chem.* **74**, 1905 (2003).
- [21] T. J. Johnson and L. E. Locascio, *Lab Chip* **2**, 135 (2002).
- [22] A. D. Stroock, S. K. W. Dertinger, A. Ajdari, I. Mezic, H. A. Stone, and G. M. Whitesides, *Science* **295**, 647 (2002).
- [23] A. Ajdari, *Phys. Rev. E* **65**, 016301 (2002).
- [24] J. L. Anderson, *Annu. Rev. Fluid Mech.* **21**, 61 (1989).
- [25] P. Mazur and J. T. Overbeek, *Recl. Trav. Chim. Pays-Bas* **70**, 83 (1951).
- [26] E. Brunet and A. Ajdari, *Phys. Rev. E* **69**, 016306 (2004).
- [27] R. J. Hunter, *Zeta Potential in Colloid Science* (Academic Press, London, 1981).
- [28] J. I. Molho, A. E. Herr, B. P. Mosier, J. G. Santiago, T. W. Kenny, R. A. Brennen, G. B. Gordon, and B. Mohammadi, *Anal. Chem.* **73**, 1350 (2001).
- [29] D. C. Tretheway and C. D. Meinhart, *Phys. Fluids* **14**, L9 (2002).
- [30] P. Joseph and P. Tabeling, *Phys. Rev. E* **71**, 035303(R) (2005).
- [31] E. Lauga, *Langmuir* **20**, 8924 (2004).
- [32] A. D. Stroock, S. K. Dertinger, G. M. Whitesides, and A. Ajdari, *Anal. Chem.* **74**, 5306 (2002b).